Egypt. J. Chem. **Vol. 64,** No. 5 pp. 2355 - 2367 (2021)

Egyptian Journal of Chemistry

http://ejchem.journals.ekb.eg/

Thermodynamic studies on the adsorption of phenol from aqueous solution by coffee husk activated carbon

Huu Son Ta,[a] Khu Le Van*[,a], Thu Thuy Luong Thi,[a] Dinh Hung Nguyen[b]

[a]*Faculty of Chemisty, Hanoi National University of Education, 136 Xuan Thuy, Cau Giay, Hanoi 100000, Vietnam*

[b] *Vinh Phuc Gifted High School, Vinh Yen City, Vinh Phuc 15000, Vietnam*

Abstract

Activated carbons (ACs) obtained from coffee husk by KOH activation at 650 (ACK-650) and 750ºC (ACK-750), were used as an adsorbent for the adsorption of phenol from aqueous solution. The ACs was characterized by SEM, EDX, BET, and Boehm titration techniques. The experimental equilibrium data of phenol adsorption was analyzed by eight isotherm models, which are four two-parameter equations (Langmuir, Freundlich, Elovich, and Temkin) and four three-parameter equations (Redlich-Peterson, Sips, Radke-Prausnitz, and Tóth). The results reveal that in general, three-parameter isotherms can provide better prediction than two-parameter isotherms. The best fit for ACK-650 sample is Sips isotherm, while for ACK-750 sample is Redlich–Peterson isotherm. Isosteric heat and thermodynamic parameters ΔG^o, ΔH^o, and ΔS^o of the adsorption were determined, and the results showed that the adsorption of phenol was exothermic and physical in nature. A scale-up of a batch system is designed for 2 to 10 L phenol with an initial concentration of 100 mg L^{-1}.

Keywords: activated carbon; isotherms; isosteric heat; phenol adsorption; thermodynamics

1. Introduction

Improving water quality is one of the major environmental challenges. Phenol is widely used in many chemical industries, like petroleum refinery, leather, plastic, pharmaceutical, paint, rubber, pesticides, and textile dyeing. Phenolic compounds are highly carcinogenic and threaten both human health and the environment, even at low concentrations. Several researches revealed that some phenolic compounds are refractory to conventional treatment [1, 2]. Therefore, phenol is one of the most detected pollutants in wastewater [3]. The World Health Organization (WHO) recommends that the highest desirable concentration of phenol in potable water is 0.001 mg L^{-1} [4]. Numerous techniques are being employed to eliminate phenolic compounds from wastewater, such as photocatalytic degradation, ozonation, extraction, biological method, adsorption, membrane-based separation, and ion exchange [5]. Nevertheless, at low contaminant concentration and large wastewater volume, the adsorption technique is one of the most effective methods [6]. Various adsorbents have been investigated for the removal of phenol from water, namely PANI [7], bentonite [8], zeolite [9, 10], carbon xerogels [11], gel [12], scoria stone [13], crab shell chitosan [14], and coal [15].

Activated carbon is considered a good phenol adsorbent due to its large surface area, high porosity, and numerous surface functional groups. Activated carbon from agricultural waste can reduce operational cost tremendously and have been investigated extensively during the last decades, such as activated carbon from tea waste [16], acai seed [17], bael fruit shell [18], *Borassus flabellifer* fruit husk [19], oil palm shell [20], and *Toona sinensis* leaves [21]. In this study, coffee husk was used to produce activated carbon using KOH activation owing to the abundance of precursors in Vietnam, the second-largest exporting coffee country in the world.

*Corresponding author e-mail: khulv@hnue.edu.vn.
Receive Date: 15 May 2020, Revise Date: 18 January 2021, Accept Date: 22 February 2021
DOI: 10.21608/EJCHEM.2021.30318.2648

The utmost desire of all academic research is to understand and predict the adsorption mechanism, then effectively design of industrial adsorption system. Therefore, it is crucial to know the distribution and the interaction between adsorbate and adsorbent through the use of the best-fit isotherm model. There are numerous methods to modeling and evaluating the experimental data, from one-parameter to five-parameter isotherms, using linear regression or nonlinear regression as well as different error analyses. In general, the more parameter used, the better fit the isotherm is. However, it is easier to use fewer parameter isotherm with linear regression. In order to evaluate the isotherm models, the following conditions must be fulfilled: (i) the fitness between the experimental and the predicted value using error analysis and (ii) the correlation between the obtained maximum adsorption capacity with the experimental adsorbed amounts at equilibrium (at the plateau of q_e ~ C_e curve).

This work aims at investigating the capability of four two-parameter models and four three-parameter models in describing the adsorption of phenol onto coffee husk activated carbon. The thermodynamic parameters and the isosteric heat of the adsorption process were examined. Scale-up batch adsorption with the volume of aqueous phenol solution from 2 to 10 L was designed, according to the best-fitted isotherm models.

2. Experimental

2.1. Materials and method

Activated carbons were prepared from Arabica coffee husks, which were collected from a coffee mill in Mai Son-Son La Province of Vietnam by KOH activation followed the same procedure as our previous work [22]. In brief, the coffee husks were washed, dried, and carbonized at 450^{o}C in the presence of nitrogen. Then the carbonized products were impregnated with KOH (weight ratio 1/3) and heated at 400^{o}C for 20 minutes under nitrogen atmosphere. After that, it was increased to 650°C (ACK-650) or 750^{o}C (ACK-750) and maintained for 60 min. Finally, the activated products were neutralized by 0.1 M HCl and washed with hot distilled water to pH 6.6÷7.0. The washed AC samples were then dried under vacuum at 120^{o}C for 24h.

Phenol crystals (purity > 99%) were supplied by Xylong Chemical, China. Phenol stock solution was prepared within 2 hours prior to use by dissolving phenol crystals in double-distilled water. The investigational solution of various concentrations was obtained by dilution of the stock solution without pH adjustment.

2.2. Characterization of activated carbons

Surface morphology of the AC samples were obtained with a field emission scanning electron microscope (S4800-Hitachi). The chemical composition of the prepared AC samples was conducted using an EDX-LE VIOEL 6610 LV (Jeol). Surface functional groups of the ACs were evaluated by Boehm titration method [23].The surface area and pore texture of AC samples were determined by N_2 adsorption isotherms at 77 K using a Micromeritics TriStar 3020 analyzer.

2.3. Phenol adsorption experiments

In adsorption isotherm studies, 100 mg of AC samples (which have been grounded and sieved by mesh #100 and #50 to particle size range 0,15 < d < 0,3 mm) was added into 100 mL of phenol solution with different initial concentrations (45 - 250 mg L^{-1}) in 250 mL Erlenmeyer flasks. The mixture was kept in an isothermal shaker (120 rpm) for 24h to reach equilibrium. After filtrated, the equilibrium concentrations of phenol in the solution were determined according to APHA standard methods [24]. The amount of phenol adsorption at equilibrium, q_e (mg g^{-1}), was calculated by:

$$q_e = \frac{(C_o - C_e)V}{m} \quad (1)$$

where C_o and C_e (mg L^{-1}) are the concentration of phenol at initial and equilibrium, respectively, V (L) is the volume of the solution, and m (g) is the mass of dry adsorbent used. In all calculations, the mean values of triplicate experiments of adsorption were used.

3. Results and discussion

3.1. Physicochemical characterization of activated carbon

SEM and EDX techniques were used to observe the surface morphologies and analyze the element weight percentage of the AC samples prepared from different activation temperatures. It can be seen from the microstructure of ACK-650 and ACK-750 in Fig. 1 that the AC samples contain numerous particles in various shapes and sizes. The ACK-750 sample presents more cracks, crevices, and high porosity than the AC-650 sample. Elemental analysis results in Table 1 show a high carbon and oxygen contents and low content of S and Cl. The carbon content of AC samples is more than 87% and the oxygen content is in the range of 11.80-12.13%. There is no trace of other elements, suggesting the effectiveness of the preparation of activated carbon from coffee husk.

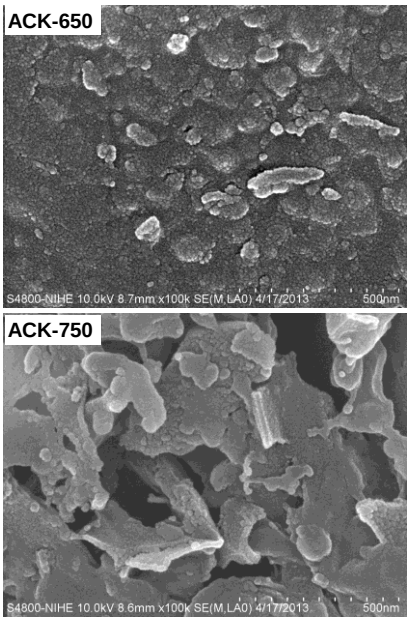

Fig. 1. SEM images of the AC samples.

The surface functional groups of the prepared AC were detected using the Boehm titration method, and the results are shown in Table 2. As can be seen, the AC prepared with KOH as activation agent present both acidic and basic surface functional groups. The amount of acidic groups is always higher than the basic groups, as result the ratio of the numbers of acidic to basic groups is equal to 2.6. At the increase of activation temperature, the number of acidic groups decreases from 2.23 to 1.73 mmol g^{-1} and the amount of basic groups diminishes from 0.86 to 0.65 mmol g^{-1}. The fast decrease in the amount of acidic group might be due to the low decomposition temperature of acidic groups (lower than 500°C) compared to basic groups (650 -980°C) [25, 26].

Table 1

Element analysis of the AC samples

Sample	Elemental Weight %				
	C	O	S	Cl	Total
ACK-650	87.37	12.13	0.26	0.24	100
ACK-750	87.99	11.80	0.21	0.23	100

Fig. 2a shows the adsorption/desorption isotherms of N_2 at 77K of ACK-650 and ACK-750 samples. The isotherms are type I according to the IUPAC classification with no hysteresis loop, indicating the presence of predominant micropores of the material [27]. The amount of nitrogen adsorbed of ACK-750 is higher than that of ACK-650, suggesting that the larger specific surface area of ACK-750 sample.

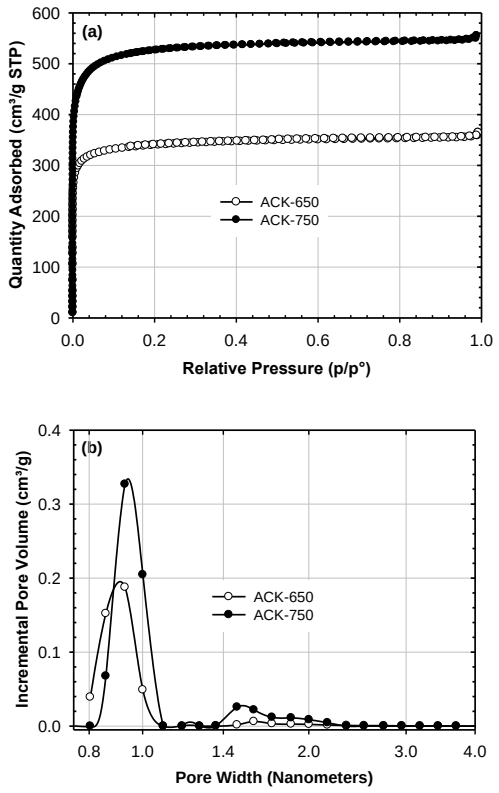

Fig. 2. a) Adsorption-desorption isotherms of N_2 at 77K of the AC samples; b) Pore size distribution of the AC samples.

Table 3. Surface area and pore texture of the AC samples.

Sample	S_{BET} (m^2 g^{-1})	S_{mic} (m^2 g^{-1})	S_{ext} (m^2 g^{-1})	S_{mic}/S_{BET} (%)	V_{mic} (cm^3 g^{-1})	V_{mes} (cm^3 g^{-1})	V_{mic}/V_{tot} (%)
ACK-650	1216	1198	18	98.52	0.5281	0.0293	94.74
ACK-750	1905	1891	14	99.27	0.8252	0.0361	95.81

The calculated specific surface area, S_{BET}, (by applying the BET equation), micropore surface area, S_{mic}, micropore volume, V_{mic}, external surface area, S_{ext} (by applying t-plot method), mesopore volume, V_{mes}, (by applying BJH method) [27] and total pore volume, V_{tot}, ($V_{tot} = V_{mic} + V_{mes}$) are summarized in Table 3. As predicted by the adsorption/desorption isotherms of N_2, S_{BET} and V_{tot} of ACK-750 (1905 m^2 g^{-1} and 0.8613 cm^3 g^{-1}) are both larger than that of ACK-650 (1216 m^2 g^{-1} and 0.5574 cm^3 g^{-1}). This result is consistent with the results obtained by SEM, in which the ACK-750 sample has a greater porosity than the ACK-650 sample. It also can be seen from Table 3 that all the samples contain mostly micopores with the percentage of micropore surface area and pore volume of the two samples are over 98% and 94%, respectively.

The pore size distribution (PSD), calculated by DFT method [27] based on nitrogen adsorption isotherms of AC sample is illustrated in Fig. 2b. Clearly, the main pore width is below 2 nm, with a majority in the range of 0.8-1.1 nm. Increasing the activation temperature from 650 to 750°C resulted in a major increase in micropores. This result is in accord with and support the result in Table 3.

3.2. Phenol adsorption equilibrium isotherms

The phenol uptakes at four different adsorption temperatures (10, 20, 30, and 40°C) of AC samples under study are displayed in Fig 3. As shown in Fig. 3, phenol-adsorbed amounts increase as phenol concentration increases, rather sharply in the low-concentration region, and more smoothly at higher concentration. The adsorptive of phenol decreases with the increasing of adsorption temperature, suggesting that phenol adsorption onto activated carbon is an exothermic process, and there exists a poor chemical reaction interplay between adsorbate and surface functionalities of ACs [28]. At all temperatures studied, the adsorption capacities of ACK-750 sample are always higher than that of ACK-650 sample, which might be due to the developed surface area and pore volume of ACK-750 sample. Besides, all the isotherms display no plateau, indicating unsaturated adsorption at the investigated conditions.

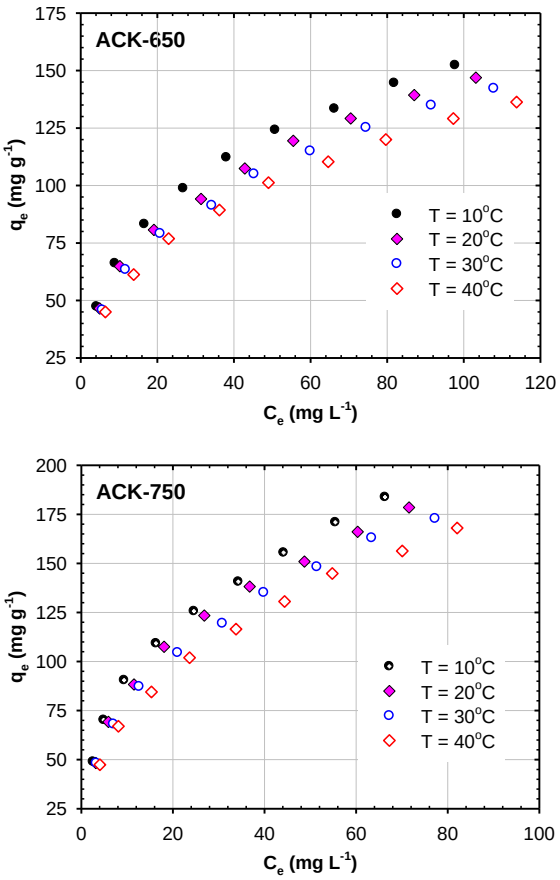

Fig. 3. Phenol uptakes at different adsorption temperature for ACK-650 and ACK-750.

The theoretical maximum monolayer coverage capacity of AC samples ($q_{m,theoretical}$) can be estimated from the specific surface area (S_{BET}) using the following equation:

$$q_{m,theoretical} = \frac{S_{BET} M}{\sigma N_A} \qquad (2)$$

where σ is the surface area of phenol molecule (30.49×10^{-20} m^2 [29]), N_A is Avogadro's constant (6.02×10^{23} mol^{-1}), M is the molar mass of phenol (94.11 g mol^{-1}), and S_{BET} is specific surface area (m^2 g^{-1}).

Table 4

Isotherm models and the parameters involved

Isotherm	Non-linear form	Linear form	Parameters	Ref
Langmuir	$q_e = \frac{q_m K_L C_e}{1+K_L C_e}$	$\frac{C_e}{q_e} = \frac{1}{q_m K_L}\frac{1}{C_e} + \frac{1}{q_m}$	q_m: maximum monolayer coverage capacity K_L: Langmuir isotherm constant	[29, 30]
Freundlich	$q_e = K_F C_e^{1/n}$	$\ln q_e = \frac{1}{n}\ln C_e + \ln K_F$	K_F: Freundlich isotherm constant n: parameter related with multiple layer coverage	[29, 31]
Elovich	$\frac{q_e}{q_m} = K_E C_e \exp\left(-\frac{q_e}{q_m}\right)$	$\ln\frac{q_e}{C_e} = -\frac{q_e}{q_{mE}} + \ln K_E q_m$	q_m: maximum monolayer coverage capacity K_E : Elovich equilibrium constant	[29]
Temkin	$q_e = B\ln(K_T C_e)$	$q_e = B\ln K_T + B\ln C_e$	B: Temkin isotherm constant K_T: the equilibrium binding constant	[29]
Redlich–Peterson	$q_e = \frac{AC_e}{1+BC_e^{\beta}}$	-	A, B: Redlich–Peterson isotherm constant β: Redlich–Peterson model exponent	[31, 32]
Sips	$q_e = \frac{q_{mS} K_S C_e^{m_S}}{1+K_S C_e^{m_S}}$	-	q_{mS}: Sips maximum adsorption capacity K_S: Sips equilibrium constant m_S: Sips model exponent.	[31]
Radke–Prausnitz	$q_e = \frac{q_{mRP} K_{RP} C_e}{(1+K_{RP} C_e)^{m_{RP}}}$	-	q_{mRP}: Radke–Prausnitz maximum adsorption capacity K_{RP}: Radke–Prausnitz equilibrium constants. m_{RP}: Radke–Prausnitz model exponent	[32]
Tóth	$q_e = \frac{q_{mTh} C_e}{(1/K_{Th} + C_e^{m_{Th}})^{1/m_{Th}}}$	-	q_{mTh}: Tóth maximum adsorption capacity K_{Th}: Tóth equilibrium constant m_{Th}: Tóth model exponent	[29, 31]

The calculated $q_{m,theoretical}$ of ACK-650 and ACK-750 samples are 623.47 and 976.74 mg g^{-1}, respectively. The higher $q_{m,theoretical}$ value of ACK-750 sample is due to the large specific surface area of ACK-750 sample compared to that of ACK-650 sample, which is 1216 and 1905 m^2 g^{-1}, respectively. The $q_{m,\ theoretical}$ is much higher than the highest experimental adsorbed amounts at equilibrium (q_e at the highest C_e of each sample), indicating that not all surface areas of activated carbons are accessible to phenol molecules.

The correlation between the amount of adsorption at equilibrium and the liquid phase concentration was evaluated using eight isotherm models, which are i) two-parameter isotherm models given by Langmuir, Freundlich, Elovich, and Temkin and ii) three-parameter isotherm models given by Redlich–Peterson, Sips, Radke–Prausnitz, and Tóth. The expressions of these isotherms are listed in Table 4. These parameters were obtained using Microsoft Excel software version 2003 for Windows. For the two-parameter models, the linear forms of the isotherm models were applied to the experimental values of q_e and C_e by employing add trend line tool. While for the three-parameter models, the non-linear regression analysis of experimental data was employed by using the solver tool [33], in which the minimizing of the root mean square error (RMSE) is performed. In all cases, the coefficient of determination (R^2) was used to evaluate the correlation between experimental data and isotherm equation, the average relative errors (ARE) was used to estimate the fit between the experimental and predicted values for adsorption capacity. RMSE, R^2, and ARE were calculated according to equations (3), (4), and (5), respectively.

$$RMSE = \sqrt{\frac{1}{N}\sum_{i=1}^{N}\left(q_{e,pre} - q_{e,mes}\right)_i^2} \quad (3)$$

$$R^2 = 1 - \frac{\sum_{i=1}^{N}(q_{e,mes} - q_{e,pre})_i^2}{\sum_{i=1}^{N}(q_{e,mes} - q_{e,mean})_i^2} \quad (4)$$

$$ARE = \frac{100}{N}\sum_{i=1}^{N}\left|\left(\frac{q_{e,pre} - q_{e,mes}}{q_{e,mes}}\right)_i\right| \quad (5)$$

where $q_{e,mes}$, $q_{e,pre}$ and $q_{e,mean}$ are the experimental, predicted, and average adsorption capacities,

respectively; N is the number of experimental data.

Modeling of adsorption isotherms by two-parameter models

The parameters of the Langmuir, Freundlich, Elovich, and Temkin equation for the phenol adsorption on the AC samples under study at different temperatures were calculated and reported in Table 5. The Langmuir isotherm applies to monolayer surface coverage adsorption, while the Freundlich model describes heterogeneous adsorptive energies on the adsorbent surface [29]. The Elovich model implies the chemisorption behavior between adsorbent and adsorbate. The Temkin isotherm model covers the effects of interactions between adsorbate/adsorbate during the adsorption process and only valid for an intermediate concentration range. As can be seen from this table:

i) The Elovich isotherm shows a relatively high coefficient of determination ($0.9768 \leq R^2 \leq 0.9922$), indicating that the linear form of this model fits well with experimental data. However, the calculated maximum monolayer coverage capacity (q_m) is much lower than the highest experimental adsorbed amounts at equilibrium (q_e at the highest C_e of each sample). Furthermore, q_e is even lower than the plateaus of the adsorption isotherms. Therefore in this study, the Elovich model is inappropriate to describe the adsorption of phenol onto ACs.

ii) For Freundlich model, the values of correlation coefficient R^2 (0.9940-0.9986) are nearest to 1, and the reported average relative errors are also the lowest (1.06-2.53), indicating that Freundlich isotherm is more suitable for describing the experimental data.

iii) Regarding the coefficient of determination ($0.9855 \leq R^2 \leq 0.9892$ for ACK-650 and $0.9812 \leq R^2 \leq 0.9849$ for ACK-750), Langmuir isotherm model is adequate to fit the experimental data. Nevertheless, ARE is in the range of 6.18 ~ 8.82 %, which is a relatively high error. Basically, due to its mathematical simplicity in linear regression and its effectiveness in evaluating adsorbent capacity (through maximum monolayer coverage capacity, q_m) and determining the feasibility of the adsorption process (by using the separation factor, R_L), the Langmuir isotherm model is extensively used in adsorption study. Thus, for comparison, the parameters obtained from Langmuir isotherm is still used with the acceptance error of about 9% ARE.

From Langmuir isotherm, R_L can be calculated by the following equation [34]:

$$R_L = \frac{1}{1 + K_L C_o} \quad (6)$$

where K_L is the Langmuir constant and C_o is the initial concentration of the phenol in solution. All the calculated separation factors for phenol adsorption on ACK-650 and ACK-750 samples are less than 1 and greater than zero, indicating favorable adsorption.

The maximum adsorption capacities, q_m, obtained from Langmuir isotherms for both AC samples (158.15-171.56 mg g^{-1} for ACK-650 sample and 196.58-205.63 mg g^{-1} for ACK-750 sample) are less than the theoretical q_m values, whereas in the similar range as the highest experimental adsorbed amounts at equilibrium (q_e at the highest C_e of each sample), and is comparable with other researches (142.9 mg g^{-1} on AC from tea industry waste [16], 156.25 mg g^{-1} on AC from waste tyres [34]). In all cases, q_m values of ACK-750 sample are always higher than that of ACK-650 sample. According to V. Fierro [35], phenol adsorption is controlled by micropore volume and the ratio of acidic to basic surface functional groups. Since the two AC samples have the same ratio of acidic to basic groups (equal to 2.6), the difference in q_m might be due to the divergence in specific surface area and micropore volume of the ACK-750 sample (1905 m^2 g^{-1} and 0.8252 cm^3 g^{-1}) to the ACK-650 sample (1216 m^2 g^{-1} and 0.5281 cm^3 g^{-1}). Furthermore, q_m slightly decreased with increasing adsorption temperature, q_m decreased from 171.56 to 158.15 mg g^{-1} for ACK-650 sample, and from 205.63 to 196.58 mg g^{-1} for ACK-750 sample when the adsorption temperature increased from 10 to 40°C.

iv) The Temkin equation has R^2 in the range of 0.9803-0.9869 for ACK-650 sample, and of 0.9742-0.9828 for ACK-750 sample. These values of R^2 are far from 1, compared to that of Langmuir isotherm. However, ARE values calculated from this model (in the range of 3.85-4.43 for ACK-650 sample and in the range of 5.00-5.93 for ACK-750 sample) are less than ARE value from Langmuir model (6.16-7.37 for ACK-650 sample and 7.82-8.82 for ACK-750 sample). This result shows that, in terms of fitting between experimental data and isotherm equation, the Langmuir model can describe better. However, regarding the correlation between the experimental and the predicted values, the Temkin model is more suitable.

Table 5

Parameters of the Langmuir, Freundlich, Elovich, and Temkin isotherms for the adsorption of phenol onto activated carbon at different temperatures

Model	Parameters	Sample							
		ACK-650				ACK-750			
		10ºC	20ºC	30ºC	40ºC	10ºC	20ºC	30ºC	40ºC
Langmuir	q_m (mg g^{-1})	171.56	167.95	163.93	158.15	205.63	203.21	199.20	196.58
	K_L(L mg^{-1})	0.061	0.051	0.047	0.043	0.083	0.071	0.063	0.054
	R^2	0.9892	0.9855	0.9855	0.9874	0.9819	0.9849	0.9813	0.9812
	ARE (%)	7.37	7.73	7.16	6.18	8.82	7.82	8.3	7.96
Freundich	K_F ($mg^{1-1/n}$ $L^{1/n}$ g^{-1})	29.249	26.406	24.4	22.419	36.319	32.409	30.788	27.351
	n	2.739	2.681	2.638	2.606	2.58	2.487	2.501	2.421
	R^2	0.9972	0.9968	0.9976	0.9985	0.9940	0.9943	0.9986	0.9984
	ARE (%)	1.83	1.36	1.41	1.06	2.41	2.53	1.30	1.21
Elovich	q_m (mg g^{-1})	53.22	53.84	53.79	52.82	66.85	69.17	67.66	69.63
	K_E(L mg^{-1})	0.478	0.373	0.318	0.277	0.561	0.423	0.386	0.294
	R^2	0.9922	0.9822	0.9828	0.9875	0.9817	0.9874	0.9770	0.9768
Temkin	B (mg g^{-1})	33.45	33.14	32.80	32.09	40.23	40.79	39.62	39.88
	K_T(L mg^{-1})	0.829	0.683	0.595	0.521	1.109	0.878	0.814	0.651
	R^2	0.9869	0.9803	0.9809	0.9838	0.9763	0.9828	0.9742	0.9745
	ARE (%)	3.85	4.43	4.24	4.20	5.27	5.00	5.87	5.93

From Temkin isotherm constant, B, the variation of adsorption energy can be calculated based on the following equation [29, 36]:

$$B = \frac{q_m RT}{\Delta Q} \qquad (7)$$

where q_m is maximum monolayer coverage capacity, R is gas constant, T is temperature, and ΔQ is a variation of adsorption energy.

The calculated ΔQ values from equation (7) with q_m from Langmuir isotherms are shown in Table 6. All the calculated ΔQ is positive, and ΔQ = - ΔH [29], therefore it can be deduced that the adsorption process is exothermic. This result is consistent with the inference when observing adsorption isotherms at different temperatures as presented above. ΔQ is in the range of 12.07 – 12.83 kJ mol^{-1} for ACK-650 sample and of 12.03 – 12.83 kJ mol^{-1} for ACK-750 sample. This result is comparable to the one obtained by Oualid Hamdaoui and Emmanuel Naffrechoux [29] (ΔQ = 12.16 kJ mol^{-1}) when investigating the phenol adsorption on commercially granular activated carbon.

Table 6

ΔQ for the adsorption of phenol onto activated carbon at different temperatures.

Sample	ΔQ (kJ mol^{-1})			
	10ºC	20ºC	30ºC	40ºC
ACK-650	12.07	12.35	12.59	12.83
ACK-750	12.03	12.14	12.66	12.83

The comparison of the experimental and the predicted adsorption isotherms of phenol onto AC samples at 30ºC, according to Langmuir, Freundlich, and Temkin equations is showed in Fig. 4. It can be seen that the Freundlich curve passes through all the experimental data, the Temkin curve is much closer to the experimental than the Langmuir curve. The observation from Fig. 4 and the above discussion can affirm that the adsorption isotherm models fitted the data in the following order: Freundlich > Temkin > Langmuir isotherms.

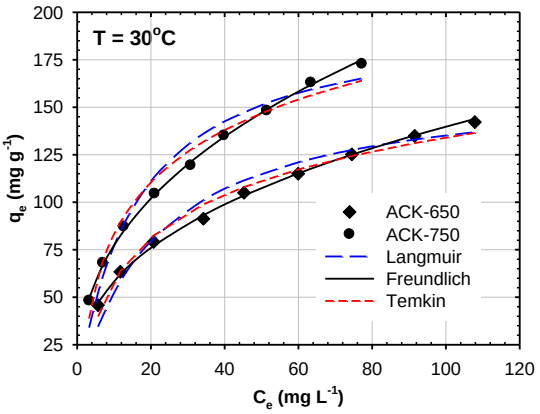

Fig. 4. Comparison of the experimental and the predicted adsorption isotherms of phenol onto AC samples at 30ºC according to Langmuir, Freundlich, and Temkin equations.

Modeling of adsorption isotherms by three-parameter models

The four three-parameter isotherms were used to interpret the phenol adsorption equilibrium, namely Redlich-Peterson isotherm, Sips isotherm, Radke–Prausnitz isotherm, and Tóth isotherm (Table 4). All

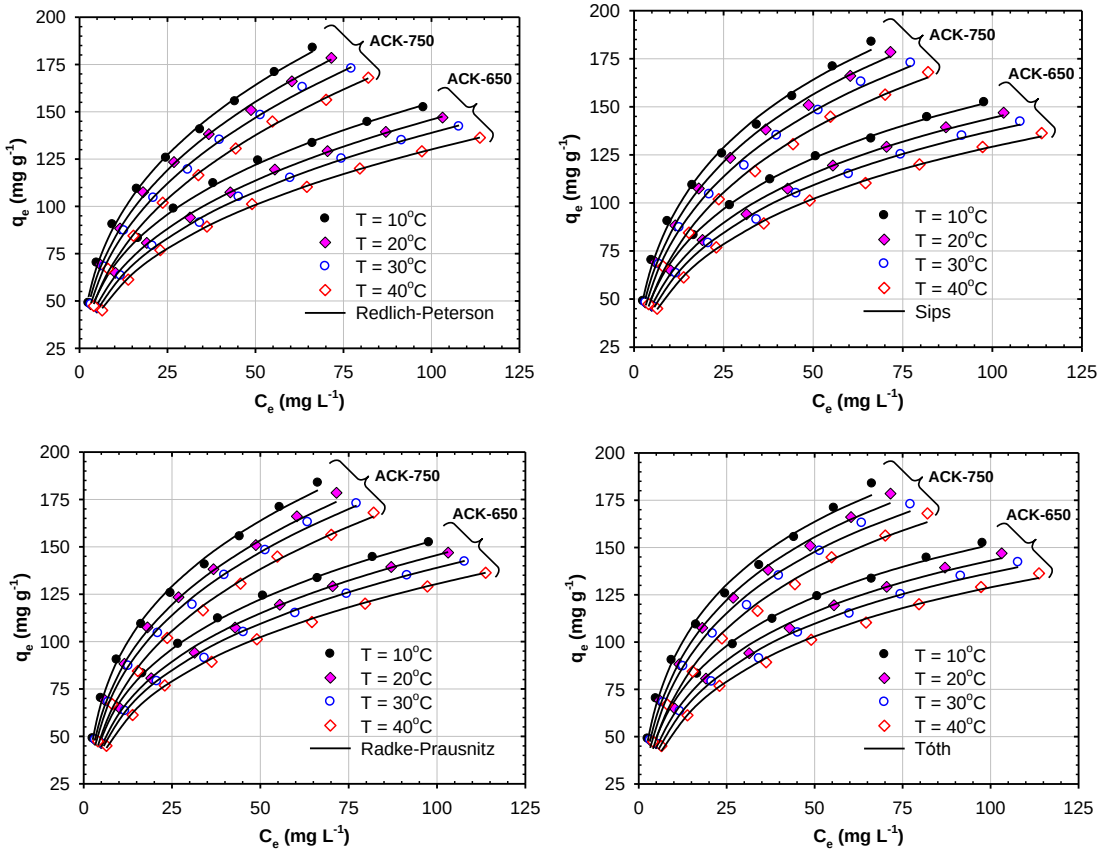

Fig. 5. Comparison of experimental and predicted adsorption isotherms of phenol onto AC samples at different adsorption temperature according to Redlich–Peterson, Sips, Radke-Prausnitz, and Tóth models.

Table 7

Parameters of the Redlich–Peterson, Sips, Radke-Prausnitz, and Tóth isotherms for the adsorption of phenol onto activated carbon at different temperatures.

Model	Parameters	Sample							
		ACK-650				ACK-750			
		10ºC	20ºC	30ºC	40ºC	10ºC	20ºC	30ºC	40ºC
Redlich–Peterson	A (L g^{-1})	154.88	139.47	124.70	111.51	187.83	179.58	163.109	144.63
	B(L mg^{-1})$^{\beta}$	4.637	4.761	4.598	4.415	4.475	4.765	4.716	4.724
	β	0.665	0.649	0.643	0.641	0.647	0.634	0.626	0.611
	R^2	0.9988	0.9988	0.9986	0.9992	0.9980	0.9980	0.9990	0.9991
	ARE (%)	1.08	1.17	1.20	0.90	1.96	1.72	0.99	1.06
Sips	q_{mS} (mg g^{-1})	384.79	375.74	359.38	351.10	484.09	462.33	453.17	433.97
	$K_S\left(\text{L mg}^{-1}\right)^{m_S}$	0.071	0.064	0.061	0.057	0.073	0.067	0.062	0.055
	m_S	0.484	0.494	0.504	0.506	0.499	0.520	0.526	0.546
	R^2	0.9996	0.9976	0.9973	0.9988	0.9964	0.9975	0.9975	0.9975
	ARE (%)	0.52	1.16	1.10	0.89	2.18	1.74	1.74	1.80
Radke–Prausnitz	q_{mRP} (mg g^{-1})	44.17	42.07	40.35	38.37	54.86	50.57	48.48	46.07
	K_{RP} (L mg^{-1})	0.558	0.493	0.475	0.435	0.691	0.620	0.579	0.494
	m_{RP}	0.687	0.678	0.676	0.672	0.686	0.671	0.663	0.649
	R^2	0.9987	0.9975	0.9972	0.9988	0.9968	0.9973	0.9973	0.9976
	ARE (%)	1.32	1.55	1.19	1.03	1.90	1.44	1.79	1.98
Tóth	q_{mTh} (mg g^{-1})	415.13	393.83	376.83	365.83	502.18	475.98	455.83	423.83
	$K_{Th}\left(\text{L mg}^{-1}\right)^{m_{Th}}$	0.656	0.567	0.519	0.490	0.654	0.558	0.513	0.424
	m_{Th}	0.309	0.327	0.337	0.340	0.322	0.343	0.354	0.382
	R^2	0.9983	0.9948	0.9947	0.9968	0.9937	0.9960	0.9937	0.9936
	ARE (%)	1.44	2.30	2.13	1.66	2.65	2.01	2.86	3.14

these models are the modification of Langmuir equation and/or Freundlich equation with the aim of reducing the error between experimental and predicted value as well as widen the applicable concentration range. As a result, these models can describe a hybrid between monolayer sorption and multilayer sorption. The Redlich-Peterson equation reduces to Freundlich model at high adsorbate concentration and Langmuir model when Redlich-Peterson exponent β equals 1. The Sips model predicts the Freundlich model at low adsorbate concentration, but envision the Langmuir model at high adsorbate concentration. The Radke-Prausnitz isotherm gives a good fit over a wide range of adsorbate concentration. The Tóth model is the most useful in describing heterogeneous adsorption systems that satisfy both low and high-end boundaries of adsorbate concentration. The comparison of the experimental and the predicted adsorption isotherms of phenol onto AC samples at different adsorption temperatures, according to Redlich–Peterson, Sips, Radke-Prausnitz, and Tóth models is shown in Fig. 5 and summarized in Table 7. It can be seen that:

i) R^2 and ARE value of Radke–Prausnitz models are in the range of 0.9968-0.9987 and 1.03-1.98, respectively. The R^2 values are very close to 1, and ARE values are very small (< 2%). However, the q_m values calculated from this model (in the range of 38.37-44.17 mg g^{-1} for ACK-650 sample and in the range of 46.07 – 54.86 mg g^{-1} for ACK-750 sample) are lower than the adsorbed amounts at equilibrium corresponding to the plateaus of the isotherms indicating the Radke–Prausnitz isotherm cannot describe the experimental equilibrium data.

ii) R^2 values of Redlich–Peterson, Sips, and Tóth models are in the range of 0.9980-0.9992, 0.9964-0.9996, and 0.9936-0.9983. The corresponding ARE values of the three models are in the range of 0.90-1.96, 0.52-2.18, and 1.44-3.14, respectively. The q_m values calculated according to Sips model (351.10-384.79 mg g^{-1} for ACK-650 sample and 433.97-484.09 mg g^{-1} for ACK-750 sample) are greater than that of Langmuir model but smaller than that of Tóth model (365.83 - 415.13 mg g^{-1} for ACK-650 sample and 423.83 - 502.18 mg g^{-1} for ACK-750 sample). The q_m values calculated by Sips and Tóth models are less than the $q_{m,\ theoretical}$ values. Therefore, based on the error functions and the rationality of q_m value, all three models Redlich–Peterson, Sips, and Tóth can describe well the adsorption of phenol on ACK-650 and ACK-750.

iii) It also can be seen from Table 7 that ARE value is lowest when applying Redlich-Peterson model to ACK-750 while to ACK-650 sample, it is lowest when applying Sips model. The reason might be due to the difference in adsorption equilibrium concentration of phenol in two cases. q_m of ACK-750 is higher than that of ACK-650, therefore, at the same q_e, the equilibrium concentration of phenol in solution of ACK-650 adsorption experiment is higher than that in solution of ACK-750 adsorption experiment. The Sips model can avoid the limitation of increased adsorbate concentration and as a result, it can describe the experimental data effectively for higher adsorbate concentration.

Comparison between linear regression two-parameter models and non-linear regression three-parameter models

For all the six models that can describe the adsorption process of phenol onto ACK-650 and ACK-750 samples as discussed previously, based on coefficients of determination and average relative error, it can be seen that three-parameter isotherms can provide better prediction than two-parameter isotherms. This is in agreement with researches on the adsorption of phenol onto activated carbon fibers [37] or natural soils [38]. In case of ACK-650 sample, the fitting order for all the adsorption isotherm models are Sips > Redlich–Peterson > Freundlich > Tóth > Temkin > Langmuir isotherms, while in the case of ACK-750 sample, the order is Redlich–Peterson > Sips > Freundlich > Tóth > Temkin > Langmuir isotherms.

3.2. Thermodynamic studies

Thermodynamic parameters such as standard free enthalpy (ΔG^o), enthalpy (ΔH^o) and entropy (ΔS^o) of phenol adsorption were determined using the following equations:

$$\Delta G^o = - RT\ln K_o \quad (8)$$

$$\ln K_o = -\frac{\Delta H^o}{R}\cdot\frac{1}{T}+\frac{\Delta S^o}{R} \quad (9)$$

where R is the universal gas constant (8.314 J mol^{-1} K^{-1}), T is the temperature (K), and K_o is the apparent equilibrium constant.

K_o can be calculated using the equation [39]:

$$K_o = \lim_{C_e \to 0} \frac{q_e}{C_e} \quad (10)$$

where C_e (mg mL^{-1}) is the equilibrium concentration,

q_e (mg g^{-1}) is the amount of phenol adsorption at equilibrium calculated according to the Ships isotherm for ACK-650 and to the Redlich–Peterson isotherm for ACK-750 with the parameters listed in Table 8.

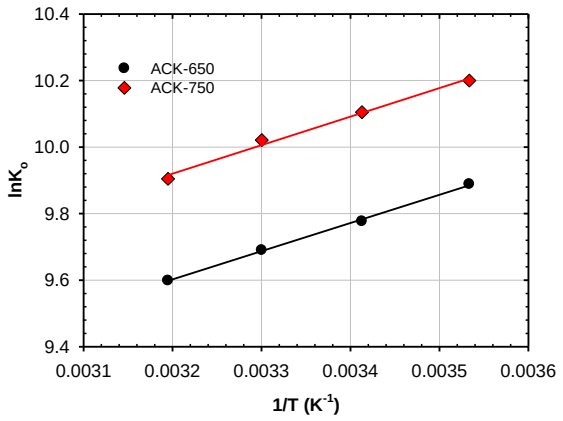

Fig. 6. Plot of $\ln K_o$ vs 1/T for ACK-650 and ACK-750.

The values of K_o is determined from the intercept by plotting $\ln(q_e/C_e)$ versus C_e and extrapolating to C_e = 0 (Fig not show). The ΔH^o and ΔS^o values can be obtained from the slope and the intercept of the plot of $\ln K_o$ versus 1/T (Fig. 6). The acquired thermodynamic parameters are given in Table 6. For all AC samples, ΔH^o and ΔG^o were negative while ΔS^o was positive. ΔG^o in the range of -23.266 to -25.775 kJ mol^{-1}, slightly larger negative than the value of physical adsorption (-20 ~ 0 kJ mol^{-1}) but not up to chemisorption range (-80 ~ -400 kJ mol^{-1}) [40], suggesting that the adsorption of phenol onto ACK-650 and ACK-750 are mainly physical adsorption and boosted by chemisorption. The chemisorption is due to the surface functional groups of AC samples, especially basic groups, which can form donor-acceptor complexes with phenol, thus contributing to phenol adsorption [28].

Table 8

Thermodynamic parameters for adsorption of phenol onto coffee husk activated carbon

Sample	T^o (C)	K_o	ΔG^o (kJ mol^{-1})	ΔH^o (kJ mol^{-1})	ΔS^o (J K^{-1} mol^{-1})
ACK-650	10	19700.5	-23.266	-7.046	57.29
	20	17616.7	-23.816		
	30	16155.2	-24.410		
	40	14744.1	-24.978		
ACK-750	10	26903.2	-23.999	- 7.130	59.66
	20	24465.0	-24.616		
	30	22493.9	-25.244		
	40	20022.3	-25.775		

ΔH^o is negative for both samples (-7.046 kJ mol^{-1} for ACK-650 and -7.130 kJ mol^{-1} for ACK-750), indicating the exothermic nature of the adsorption process, which is in agreement with the observation from Fig. 3 and the discussion in section 3.2. The values of ΔH^o lie in the range of physical adsorption (2.1 ~ 20.9 kJ mol^{-1}) [41]. ΔS^o is positive, demonstrating the increasing of randomness at the solid/solution interface. This might be due to the competition between the solvent and phenol for the active sites and also the breakage of the hydration shell of phenol molecules during the adsorption onto the AC samples [42].

3.3 Isosteric heat of adsorption

Isosteric heat of adsorption (ΔH_X) is defined as the heat of adsorption determined at a constant amount of adsorbate adsorbed and can be obtained using the Clausius–Clapeyron equation [43, 44]:

$$\frac{d \ln C_e}{dT} = -\frac{\Delta H_X}{RT^2} \qquad (11)$$

The integration form can be written as:

$$\ln C_e = \frac{\Delta H_X}{R}\frac{1}{T} + \text{const} \qquad (12)$$

The equilibrium concentration (C_e) at a constant amount of phenol adsorbed is estimated through the dependence between q_e and Ce. As presented above, the relationship between C_e and q_e is best described by the Sips equation for the ACK-650 sample and Redlich-Peterson for the ACK-750 sample and can be well described by the Freundlich equation. However, the calculation of C_e from the three-parameters model is relatively difficult. Thus, for simplicity, in this study, C_e at constant surface coverage (20, 40, 60, 80 and 100 mg g^{-1}) is calculated from the Freundlich equation:

$$\ln C_e = n(\ln q_e - \ln K_F) \qquad (13)$$

Fig. 7 presents the plots of lnCe versus reciprocal T at different q_e of ACK-650 sample (Fig. 7a) and ACK-750 sample (Fig. 7b). All the obtained plots are found to be linear. The R^2 values of the isosteres and the corresponding ΔH_X values are listed in Table 9. It can be seen that ΔH_X is negative suggesting the exothermic nature of the process. ΔH_X for the adsorption of phenol on both sample at each q_e value (between 20 and 100 mg g^{-1}) are in the same range and oscillate between -18.158 and -12.662 kJ mol^{-1} (less negative than -80 kJ

mol^{-1}), which correspond to physical adsorption process [45, 46]. This result confirms the previous conclusion in section 3.2.

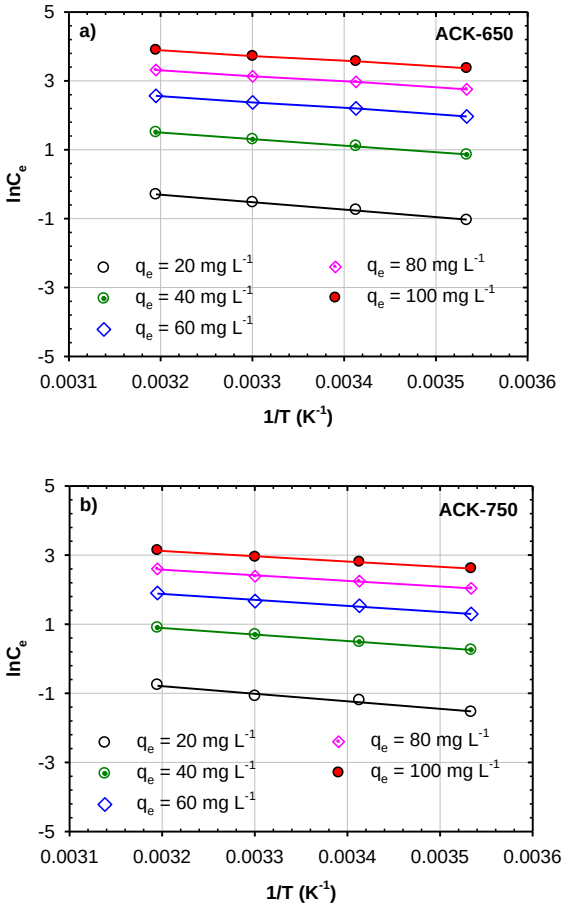

Fig. 7. Plots of ln C_e against 1/T for phenol adsorption onto ACK-650 (a) and ACK-750 (b).

Table 9

Isosteric heat of phenol adsorption on coffee husk activated carbon

No	q_e (mg g^{-1})	ACK-650		ACK-750	
		ΔH_x (kJ mol^{-1})	R^2	ΔH_x (kJ mol^{-1})	R^2
1	20	-18.074	0.9978	-18.158	0.9723
2	40	-15.810	0.9981	-15.791	0.9833
3	60	-14.486	0.9982	-14.407	0.9895
4	80	-13.546	0.9982	-13.424	0.9935
5	100	-12.818	0.9981	-12.662	0.9960

The variation of ΔH_X with different q_e is presented in Fig. 8. As can be seen from this figure, the ΔH_X values become less negative with the increase in surface loading indicating the heterogeneous surfaces of coffee husk activated carbon. The nearly linear dependence of ΔH_X on q_e might be explained due to the phenol-AC and phenol-phenol interactions. The attraction of phenol-AC interaction causes an exothermic effect while the repulsion of phenol-phenol interaction creates an endothermic effect. At higher surface coverage, the repulsion reaction between phenol-phenol increase which in turn make ΔH_X less negative.

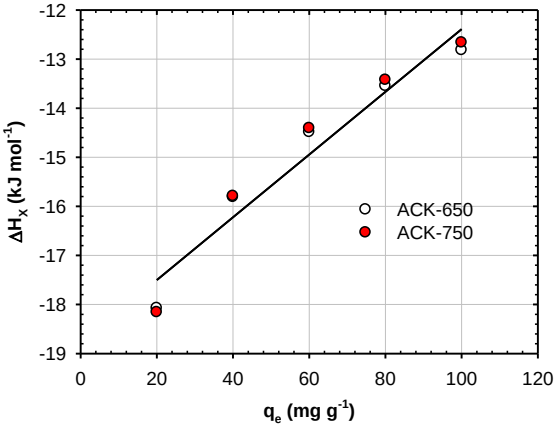

Fig. 8. Plot of isosteric heat of adsorption against surface loading for phenol adsorption onto coffee husk activated carbon.

3.3. Scale up design

The batch adsorption process is usually designed based on adsorption isotherm [47]. It is assumed that when phenol is mixed with W mass of activated carbon from coffee husk, the initial phenol concentration is decreased from C_o to C_t in solution volume V at any specific time wherein the adsorbed phenol quantity of each gram of the activated carbon is altered from q_o to q_t. When t = 0, q_o = 0, mass balance is expressed as equation (14):

$$V(C_o - C_t) = W(q_t - q_o) = Wq_t \quad (14)$$

At equilibrium $C_t = C_e$ and $q_t = q_e$, the equation (14) is modified as equation (15):

$$W = \frac{V(C_o - C_t)}{q_t} = \frac{V(C_o - C_e)}{q_e} \quad (15)$$

Using the best supportive Sips model for ACK-650 sample and Redlich–Peterson model for ACK-750 sample, the equation (15) is modified to form equation (16) and (17):

For ACK-650:

$$W = \frac{V(C_o - C_e)(1 + K_S C_e^{m_s})}{q_{mS} K_S C_e^{m_s}} \quad (16)$$

For ACK-750:

$$W = \frac{V(C_o - C_e)(1 + BC_e^{\beta})}{AC_e} \qquad (17)$$

Table 10

Weight of activated carbon (g) for the removal of phenol (%) at 20ºC for different volumes of phenol solution

V (L)	ACK-650					ACK-750				
	20%	40%	60%	80%	90%	20%	40%	60%	80%	90%
2	0.297	0.653	1.126	1.941	2.879	0.216	0.482	0.842	1.463	2.156
4	0.595	1.306	2.252	3.881	5.758	0.433	0.964	1.684	2.926	4.313
6	0.892	1.959	3.378	5.822	8.637	0.649	1.445	2.526	4.388	6.469
8	1.190	2.612	4.504	7.762	11.516	0.865	1.927	3.368	5.851	8.626
10	1.487	3.265	5.630	9.703	14.395	1.081	2.409	4.210	7.314	10.782

Using the equation (16), (17), and the parameter from Table 7, the required weight of activated carbon from coffee husk for the removal of phenol concentration of 100 mg L^{-1} at 20ºC for different volumes (2 to 10 L) of aqueous phenol solutions (wastewater or effluent) was evaluated and given in Table 10.

It can be seen from Table 10 that the weight of activated carbon needed for the removal of phenol is relatively low, even when removing more than 80% of the initial phenol concentration (~ 0,97 g L^{-1} for ACK-650 and ~ 0,73 g L^{-1} for ACK-750). In all cases, the predicted weight of ACK-750 sample is always lower than that of ACK-650 sample, which is due to the higher ability adsorption of ACK-750 sample. This result suggesting the effectiveness of activated carbon from coffee husk on the removal of phenol from wastewater.

4. Conclusion

AC samples were prepared from coffee husk by KOH activation. The obtained ACs present a developed specific surface area (1216 and 1905 m^2 g^{-1}) with predominantly microporous (94.74 – 95.81% of micropore volume) and contain numerous acidic and basic surface functional groups. Equilibrium adsorption of phenol on ACs at four temperatures was studied and modeled using eight different isotherm models. Equilibrium adsorption of phenol on activated carbon derived from coffee husk at four temperatures was studied and modeled using eight different isotherm models. The ACs possessed a high adsorption capacity to remove phenol from aqueous solutions. The Elovich and Radke–Prausnitz equations are not appropriate for the experimental results. The classification of the remaining six tested models for the description of adsorption equilibrium isotherms of phenol on activated carbon in this study are Sips > Redlich–Peterson > Freundlich > Tóth > Temkin > Langmuir for ACK-650 sample and Redlich–Peterson > Sips > Freundlich > Tóth > Temkin > Langmuir for ACK-750 sample. The variation of adsorption energy deduced from the Temkin equation was about 12.50 kJ mol^{-1}. The thermodynamic studies showed that the process was endothermic ($\Delta H^o \approx$ - 7 kJ mol^{-1}) and spontaneous (- 26 < ΔG^o < -23 kJ mol^{-1}) in nature and physical adsorption. Isosteric heat of adsorption is in the range of -18.158 and -12.662 kJ mol^{-1} while the surface loading is in the range of 20 and 100 mg g^{-1}. A scale-up of a batch system is designed for 2 to 10 L phenol with an initial concentration of 100 mg L^{-1}. It is being found that the activated carbon from coffee husk by KOH activation is a promising candidate for wastewater treatment potentially.

5. Conflicts of interest

There are no conflicts to declare.

6. References

1. Brandão, Y., et al., *Treatment of phenolic effluents by a thermochemical oxidation process (DiCTT) and modelling by artificial neural networks.* Fuel, 2013. **110**: p. 185-195.
2. Luna, A.J., et al., *Total catalytic wet oxidation of phenol and its chlorinated derivates with MnO2/CeO2 catalyst in a slurry.* Brazilian Journal of Chemical Engineering, 2009. **26**(3): p. 493-502.
3. Rodrigues, G.D., L.H.M.d. Silva, and M.d.C.H.d. Silva, *Green alternatives for sample preparation and determination of phenolic pollutants in water.* Química Nova, 2010. **33**(6): p. 1370-1378.
4. *Phenol Health and Safety Guide*, W.H. Organization, Editor. 1994: Geneva. p. 36.
5. Mohammadi, S., et al., *Phenol removal from industrial wastewaters: a short review.* Desalination and Water Treatment, 2014. **53**(8): p. 2215-2234.
6. Villegas, L.G.C., et al., *A Short Review of Techniques for Phenol Removal from Wastewater.* Current Pollution Reports, 2016. **2**(3): p. 157-167.
7. Belalia, A., A. Zehhaf, and A. Benyoucef, *Preparation of Hybrid Material Based of PANI with SiO2 and Its Adsorption of Phenol from Aqueous Solution.* Polymer Science, Series B, 2019. **60**(6): p. 816-824.

8. Ahmadi, S. and C.A. Igwegbe, *Adsorptive removal of phenol and aniline by modified bentonite: adsorption isotherm and kinetics study*. Applied Water Science, 2018. **8**(6).
9. Ba Mohammed, B., et al., *Adsorptive removal of phenol using faujasite-type Y zeolite: Adsorption isotherms, kinetics and grand canonical Monte Carlo simulation studies.* Journal of Molecular Liquids, 2019. **296**.
10. Jiang, N., et al., *Adsorption of triclosan, trichlorophenol and phenol by high-silica zeolites: Adsorption efficiencies and mechanisms.* Separation and Purification Technology, 2020. **235**.
11. Malaika, A., et al., *The impact of surface chemistry of carbon xerogels on their performance in phenol removal from wastewaters via combined adsorption-catalytic process.* Applied Surface Science, 2020. **511**.
12. Yang, Z., et al., *Imidazolium-functionalized stable gel materials for efficient adsorption of phenols from aqueous solutions.* Environmental Technology & Innovation, 2020. **17**.
13. Sharafi, K., et al., *Phenol adsorption on scoria stone as adsorbent - Application of response surface method and artificial neural networks.* Journal of Molecular Liquids, 2019. **274**: p. 699-714.
14. Francis, A.O., et al., *Equilibrium and kinetics of phenol adsorption by crab shell chitosan.* Particulate Science and Technology, 2020: p. 1-12.
15. Sun, X., et al., *Phenol adsorption kinetics and isotherms on coal: effect of particle size.* Energy Sources, Part A: Recovery, Utilization, and Environmental Effects, 2019. **43**(4): p. 461-474.
16. Gundogdu, A., et al., *Adsorption of Phenol from Aqueous Solution on a Low-Cost Activated Carbon Produced from Tea Industry Waste: Equilibrium, Kinetic, and Thermodynamic Study*. Journal of Chemical & Engineering Data, 2012. **57**(10): p. 2733-2743.
17. de Sousa Ribeiro, L.A., et al., *Preparation, characterization, and application of low-cost açaí seed-based activated carbon for phenol adsorption.* International Journal of Environmental Research, 2018. **12**(6): p. 755-764.
18. Lallan Singh, Y., M. Bijay Kumar, and A. Kumar, *Adsorption of Phenol from Aqueous Solutions by Bael Furit Shell Activated Carbon: Kinetic, Equilibrium, and Mass Transfer Studies.* Theoretical Foundations of Chemical Engineering, 2019. **53**(1): p. 122-131.
19. Sathya Priya, D. and M.V. Sureshkumar, *Synthesis of Borassus flabellifer fruit husk activated carbon filter for phenol removal from wastewater*. International Journal of Environmental Science and Technology, 2019. **17**(2): p. 829-842.
20. Lua, A.C., *A detailed study of pyrolysis conditions on the production of steam-activated carbon derived from oil-palm shell and its application in phenol adsorption.* Biomass Conversion and Biorefinery, 2019. **10**(2): p. 523-533.
21. Kong, X., et al., *Adsorption of phenol on porous carbon from Toona sinensis leaves and its mechanism.* Chemical Physics Letters, 2020. **739**.
22. Le Van, K. and T. Luong Thi Thu, *Preparation of Pore-Size Controllable Activated Carbon from Rice Husk Using Dual Activating Agent and Its Application in Supercapacitor*. Journal of Chemistry, 2019. **2019**: p. 1-11.
23. Boehm, H.P., *Surface oxides on carbon and their analysis: a critical assessment.* Carbon, 2002. **40**(2): p. 145-149.
24. *APHA Method 9221: Standard Methods for the Examination of Water and Wastewater*. 1992, American Public Health Association: America. p. 13.
25. Figueiredo, J.L., et al., *Modification of the surface chemistry of activated carbons.* Carbon, 1999. **37**(9): p. 1379-1389.
26. Shafeeyan, M.S., et al., *A review on surface modification of activated carbon for carbon dioxide adsorption.* Journal of Analytical and Applied Pyrolysis, 2010. **89**(2): p. 143-151.
27. Webb, P. and C. Orr. 1997: Norcross, Ga. : Micromeritics Instrument Corporation. 301.
28. Mojoudi, N., et al., *Phenol adsorption on high microporous activated carbons prepared from oily sludge: equilibrium, kinetic and thermodynamic studies.* Sci Rep, 2019. **9**(1): p. 19352.
29. Hamdaoui, O. and E. Naffrechoux, *Modeling of adsorption isotherms of phenol and chlorophenols onto granular activated carbon. Part I. Two-parameter models and equations allowing determination of thermodynamic parameters.* J Hazard Mater, 2007. **147**(1-2): p. 381-94.
30. Dąbrowski, A., *Adsorption — from theory to practice.* Advances in Colloid and Interface Science, 2001. **93**(1-3): p. 135-224.
31. Ayawei, N., A.N. Ebelegi, and D. Wankasi, *Modelling and Interpretation of Adsorption Isotherms.* Journal of Chemistry, 2017. **2017**: p. 1-11.
32. Hamdaoui, O. and E. Naffrechoux, *Modeling of adsorption isotherms of phenol and chlorophenols onto granular activated carbon. Part II. Models with more than two parameters.* J Hazard Mater, 2007. **147**(1-2): p. 401-11.
33. Brown, A.M., *A step-by-step guide to non-linear regression analysis of experimental data using a Microsoft Excel spreadsheet.* Computer Methods and Programs in Biomedicine, 2001. **65**(3): p. 191-200.
34. Amri, N., R. Zakaria, and A.B. Mohamad Zailani, *Adsorption of phenol using activated carbon adsorbent from waste tyres.* Pertanika Journal of Science & Technology, 2009. **17**(2): p. 371-380.
35. Fierro, V., et al., *Adsorption of phenol onto activated carbons having different textural and surface properties.* Microporous and Mesoporous Materials, 2008. **111**(1-3): p. 276-284.
36. Shikuku, V.O., et al., *Single and binary adsorption of sulfonamide antibiotics onto iron-modified clay: linear and nonlinear isotherms, kinetics, thermodynamics, and mechanistic studies.* Applied Water Science, 2018. **8**(6).
37. Juang, R.-S., F.-C. Wu, and R.-L. Tseng, *Adsorption Isotherms of Phenolic Compounds from Aqueous Solutions onto Activated Carbon Fibers.* Journal of Chemical & Engineering Data, 1996. **41**(3): p. 487-492.
38. B., S. and A. D., *Adsorption Isotherm Modeling of Phenol Onto Natural soils – Applicability of Various Isotherm Models.* International Journal of Environmental Research, 2012. **6**(1): p. 265-276.
39. Li, Q., et al., *Equilibrium, thermodynamics and process design to minimize adsorbent amount for the adsorption of acid dyes onto cationic polymer-loaded bentonite.* Chemical Engineering Journal, 2010. **158**(3): p. 489-497.
40. Yu, Y., et al., *Adsorption of water-soluble dyes onto modified resin*. Chemosphere, 2004. **54**(3): p. 425-430.
41. Liu, Y., *Is the Free Energy Change of Adsorption Correctly Calculated?* Journal of Chemical & Engineering Data, 2009. **54**(7): p. 1981-1985.
42. Li, Y.H., et al., *Adsorption thermodynamic, kinetic and desorption studies of Pb2+ on carbon nanotubes.* Water Res, 2005. **39**(4): p. 605-9.
43. Anirudhan, T.S. and P.G. Radhakrishnan, *Thermodynamics and kinetics of adsorption of Cu(II) from aqueous solutions onto a new cation exchanger derived from tamarind fruit shell.* The Journal of Chemical Thermodynamics, 2008. **40**(4): p. 702-709.
44. Srivastava, V.C., I.D. Mall, and I.M. Mishra, *Adsorption thermodynamics and isosteric heat of adsorption of toxic metal ions onto bagasse fly ash (BFA) and rice husk ash (RHA).* Chemical Engineering Journal, 2007. **132**(1-3): p. 267-278.
45. Chowdhury, S., et al., *Adsorption thermodynamics, kinetics and isosteric heat of adsorption of malachite green onto chemically modified rice husk.* Desalination, 2011. **265**(1-3): p. 159-168.
46. Doğan, M. and M. Alkan, *Removal of methyl violet from aqueous solution by perlite.* Journal of Colloid and Interface Science, 2003. **267**(1): p. 32-41.
47. Naiya, T.K., A.K. Bhattacharya, and S.K. Das, *Adsorptive removal of Cd(II) ions from aqueous solutions by rice husk ash.* Environmental Progress & Sustainable Energy, 2009. **28**(4): p. 535-546.